Available online at www.sciencedirect.com
ScienceDirect
Polymer 47 (2006) 8253–8262
polymer
www.elsevier.com/locate/polymer

The genesis of polyaniline nanotubes

Jaroslav Stejskal [a,*], Irina Sapurina [b], Miroslava Trchová [a], Elena N. Konyushenko [a], Petr Holler [a]

[a] *Institute of Macromolecular Chemistry, Academy of Sciences of the Czech Republic, Heyrovsky Sq. 2, 162 06 Prague 6, Czech Republic*
[b] *Institute of Macromolecular Compounds, Russian Academy of Sciences, St. Petersburg 199004, Russia*

Received 26 June 2006; received in revised form 26 September 2006; accepted 1 October 2006
Available online 27 October 2006

Abstract

Aniline has been oxidized with ammonium peroxydisulfate in 0.4 M acetic acid. Protons are produced in the course of oxidation and the pH decreases as the reaction proceeds. The oxidation had two subsequent phases: (1) the oxidation of the neutral aniline molecules and the initially produced low-molecular weight aniline oligomers at low acidity, followed by (2) the oxidation of the anilinium cation after the acidity became higher. The two phases of oxidation gave different products, aniline oligomers with mixed *ortho*- and *para*-coupling of aniline molecules, and polyaniline nanotubes, respectively.

The aniline oligomers are produced at first at low acidity, pH > 4, some of them as rod-like crystals. The molecular weight of the oligomers has been assessed by gel-permeation chromatography to be of several thousands. The 2–3 wt.% content of sulfur in deprotonated samples suggests that the oxidation products are partly sulfonated. The oxidation of *ortho*-coupled anilines combined with intramolecular cyclization produces phenazine units or their blocks, as indicated by FTIR spectra. A high-molecular weight polyaniline is produced at pH < 2. The protonation of the intermediate pernigraniline form of polyaniline is a prerequisite for the polymerization.

The nano-sized oligomer crystallites serve as starting templates for the nucleation of PANI nanotubes. Further growth of nanotubes proceeds by the self-organization of the phenazine units or their blocks located at the ends of the PANI chains. Polyaniline nanotubes have a typical outer diameter of 100–200 nm, with a wall thickness of 50–100 nm, an inner diameter of 0–100 nm, and a length extending to several micrometres.

Keywords: Conducting polymer; Conductivity; Polyaniline nanotubes

1. Introduction

The importance of the conducting polymers, like polyaniline (PANI) and polypyrrole, has been recognized for many years [1–3]. The observation that these polymers can produce ‘‘one-dimensional’’ morphologies, like nanotubes [4–8], nanowires [9–16] or non-spherical colloidal nanoparticles [17–22], made them the exciting object of many investigations. The polymerization of aniline on ‘‘soft’’ templates, micellar structures involving aniline or aniline salts, has been offered as an explanation for the nanotube formation [6,11,12,16]. The oxidation of pyrrole on ‘‘hard’’ templates, afforded by inorganic nanofibers [8] or crystals of pyrrole salts [21,22], has also been reported. Low concentrations of acids with respect to aniline [11,23] and the use of organic acids [5,24] have usually been needed to obtain PANI nanotubes. Under these conditions, the oxidation of aniline starts at relatively low acidity of the medium. In a previous communication [7], we have proposed that the morphology development is controlled by the acidity of the reaction mixture and the consequent protonation of aniline, the reaction intermediates, and PANI. The *process* by which PANI nanotubes are generated has not been discussed so far. In this study, we report the individual phases of aniline oxidation, demonstrate the growth of nanotubes, and propose a model for nanotube formation.

* Corresponding author. Tel.: +42 0296809351; fax: +42 0296809410.
E-mail address: stejskal@imc.cas.cz (J. Stejskal).

0032-3861/$ - see front matter © 2006 Elsevier Ltd. All rights reserved.
doi:10.1016/j.polymer.2006.10.007

2. Experimental

2.1. Oxidation of aniline

Aniline (0.2 M) was oxidized with ammonium peroxydisulfate (APS, 0.25 M) in 0.4 M acetic acid (Fig. 1). Solutions of aniline monomer and oxidant were mixed at room temperature to start the oxidation. The reaction mixture was quickly poured over silicon windows, used in FTIR spectroscopy (26 mm in diameter), and placed in separate Petri dishes. The windows were slightly raised on a support so that the reaction mixture had access to both the top and bottom sides. After specified times, based on the preliminary determination of the course of polymerization, the silicon windows were removed from the mixture. The oxidation reaction was stopped by rinsing the oxidation products deposited on the windows with water, which removed aniline and oxidant, followed by drying in air.

The residual reaction mixture left after the removal of the silicon window was poured immediately into an excess of 1 M ammonium hydroxide to stop the polymerization. The precipitate was quickly collected on a filter, thus separated from the residual monomer and oxidant, and dried in air.

2.2. Microscopy

The research-grade optical Leica DM LM Microscope, equipped with 50× Olympus objective lenses, a scanning electron microscope (SEM) JEOL 6400 and a transmission electron microscope (TEM) JEOL JEM 2000 FX have been used to characterize the morphology of the samples.

2.3. Gel-permeation chromatography

Molecular weights were assessed with a GPC/SEC apparatus using a 8 × 600 mm PLMixedB column (Polymer Laboratories, UK) operating with *N*-methylpyrrolidone and calibrated with polystyrene standards with spectrophotometric detection at the wavelength of 650 nm. The samples were dissolved in *N*-methylpyrrolidone containing 0.025 g cm^{-3} triethanolamine for deprotonation of samples, and 0.005 g cm^{-3} lithium bromide to prevent aggregation.

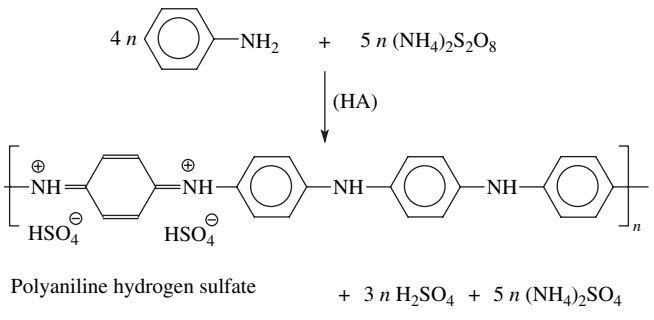

Fig. 1. The oxidation of aniline with ammonium peroxydisulfate in water yields PANI hydrogen sulfate. The *para* addition of constitutional units is shown but *ortho* addition can also be important. Sulfuric acid and ammonium sulfate or ammonium hydrogen sulfate are the by-products.

2.4. FTIR spectroscopy

Infrared spectra in the range of 400–4000 cm^{-1} were recorded at 64 scans per spectrum at 2 cm^{-1} resolution using a fully computerized Thermo Nicolet NEXUS 870 FTIR Spectrometer with a DTGS TEC detector. The spectra of the thin films deposited *in situ* on a silicon substrate were measured in the transmission mode. An absorption-subtraction technique was applied to remove the spectral features of the silicon wafers. FTIR spectra of powders were measured in the transmission mode after dispersion of the samples in potassium bromide pellets. The spectra were corrected for the presence of carbon dioxide and humidity in the optical path.

3. Results

We have recently reported [7] that the morphology of PANI, obtained after the oxidation of aniline under various acidity conditions, varies: in solutions of strong (sulfuric) acid, a common granular PANI was produced, while in solutions of weak (acetic) acid, PANI nanotubes were obtained. The internal cavity of the PANI nanotubes is easily visible in TEM micrographs (Fig. 2). Nanorods without a bore accompany

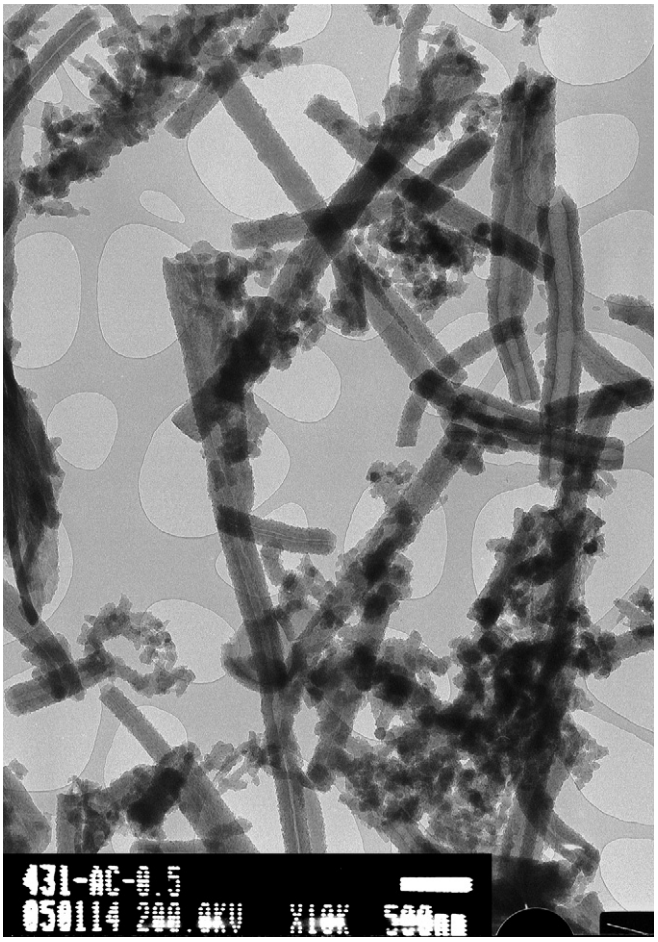

Fig. 2. TEM micrographs of PANI nanotubes and related structures.

the nanotubes. In the present paper, we concentrate on the process of nanotube formation.

3.1. The course of aniline oxidation

The oxidation of aniline is an exothermic process, and its course is easily followed by recording the reaction temperature [25,26] (Fig. 3A). The oxidation of aniline in water or in mildly acidic solution proceeds in two consecutive phases [7,25,27]. This is illustrated in the present study on the oxidation of aniline in 0.4 M acetic acid (Fig. 3A).

The oxidation of aniline starts [28] at pH 4.5 (Fig. 3B). The pK_a of aniline [25,29] is 4.6. Under such conditions, aniline exists as an approximately equimolar mixture of neutral molecules, which are easily oxidized, and anilinium cations, which are oxidized much more slowly [28]. The temperature of the reaction mixture increases as the oxidation proceeds. At the same time, the pH decreases [25,27,30], because hydrogen atoms, abstracted during the oxidation from amino groups and benzene rings, are released as protons, *i.e.*, as sulfuric acid [31–33] (Fig. 1) or hydrogen sulfate salt [25]. The pH value at the end of polymerization is 1.2.

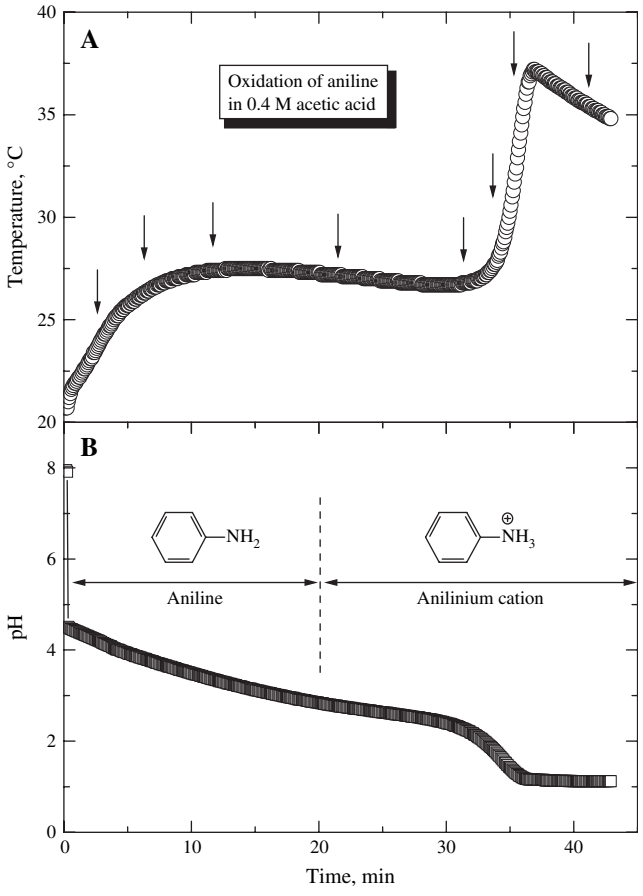

Fig. 3. (A) Temperature and (B) acidity changes during the oxidation of 0.2 M aniline with 0.25 M ammonium peroxydisulfate in 0.4 M acetic acid, started at ~22 °C. The times of sample collection are marked with arrows. The border between the predominance of neutral aniline molecules and anilinium cations is only approximate.

As the pH becomes lower than 4 (Fig. 3B), aniline molecules become protonated and convert to anilinium cations [28]. That is why the mechanism of the oxidation changes and the oxidation proceeds as in solutions of strong acids. In strongly acidic media, an athermal induction period is followed by the exothermic polymerization [25,31]. Thus, after 14 min of reaction, an induction period intervenes, which extends to 32 min (Fig. 3A).

The induction period extends this far, as the pH drops below 2, when the oxidized oligomeric intermediate, pernigraniline, becomes protonated [25,34]. The protonation of the pernigraniline form of PANI, manifested by the typical blue colour of the reaction mixture, is a prerequisite for the formation of conducting PANI of high molecular weight. We can thus conclude that the mechanism of aniline oxidation depends on whether the aniline molecules and the reaction intermediates based on aniline are protonated or not.

3.2. Evolution of nanotubes

The preparation of PANI nanotubes has been well documented [3,5,7,23]; studies related to the *process* of their formation, however, are scarce [35]. The oxidation of aniline in 0.4 M acetic acid yields products, which are insoluble in the aqueous medium. After the beginning of oxidation, they precipitate from the reaction medium as semi-crystalline oligomers, rod-like objects, which have the dimensions of several micrometres. They are easily visible by optical microscopy (Fig. 4A), and the SEM reveals details of their complex structure (Fig. 5). Only in the advanced stage of aniline oxidation, $t > 21$ min, we can observe nanotubes growing from them (Fig. 4B,C). The fact that they are nanotubes is demonstrated, in addition to TEM images (Fig. 2), also by SEM images (Fig. 6) – the internal cavity in broken nanotubes is easily visible (Fig. 6B). The typical outer diameter of nanotubes is 100–200 nm, the inner diameter is 0–100 nm.

Optical microscopy illustrates the fact that the nanotubes grow from macroscopic templates just as tree branches stem from trunks (Fig. 4B,C). There are no loose nanotubes, and the PANI structure has a connective character. This reflects the basic principle of PANI formation: chain growth beyond the dimer stage occurs in the solid-state structure that has already been produced, not in solution [36]. The granular PANI precipitate is produced close to the end of polymerization (Fig. 4D). As it sediments, it covers the nanotubular structure deposited on the silicon windows. This precipitate virtually always accompanies the nanotubes (Fig. 2).

In addition to nanotubes, other objects are also present. Nanospheres of *ca* 50 nm diameter are observed by SEM (Figs. 5A,6A). In fact, nanospheres could be in the same relation to the nanotubes, as fullerene and single-wall nanotubes are related in the realm of carbon chemistry. They are hardly discernible by optical microscopy (Fig. 4B). Our previous study [7] as well as other papers [23,37] has also shown nanospheres in TEM micrographs. Hollow PANI nanospheres were also produced when aniline was polymerized in the presence of triblock copolymers [38]. The role of the acidity of the

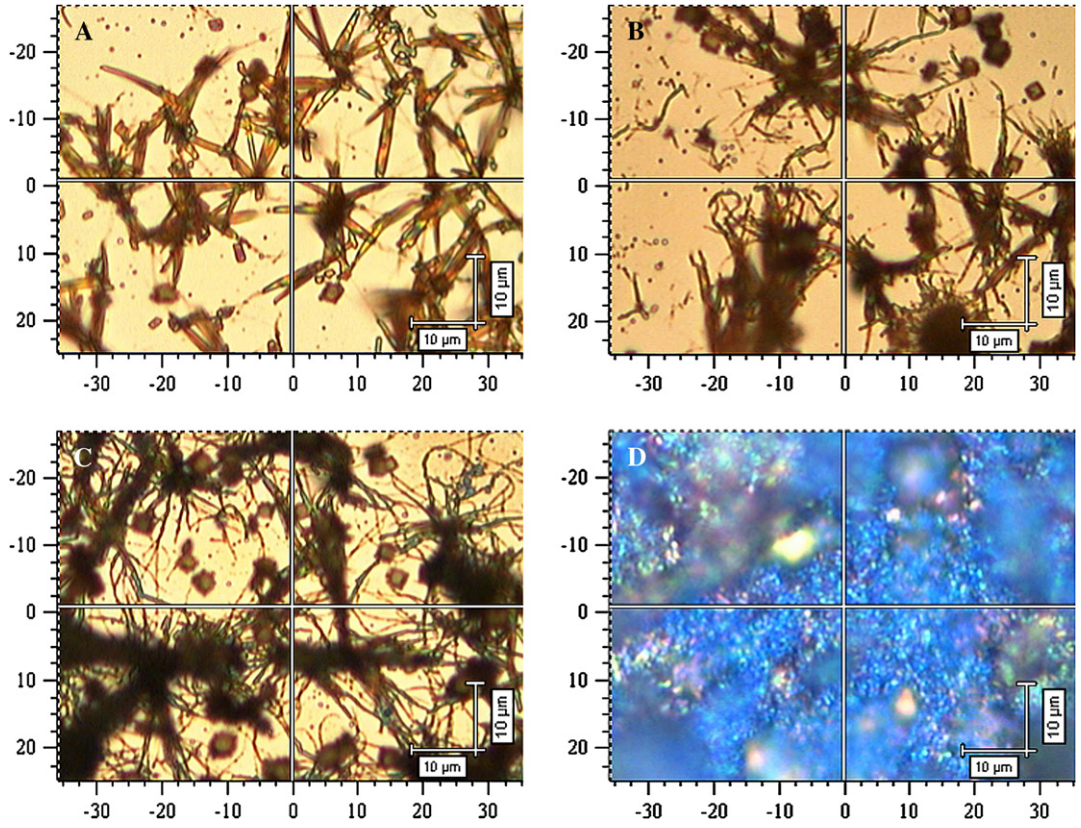

Fig. 4. Optical microscopy of the oxidation products deposited on silicon windows after reaction times t = (A) 5, (B) 21, (C) 31, and (D) 38 min.

reaction mixture in the formation of hollow PANI microspheres has also recently been reported [33].

3.3. The characterization of reaction intermediates by GPC

Samples of reaction intermediates have been collected in the course of oxidation at the times t marked by arrows in Fig. 3. The oxidation products produced at the beginning of reaction are the oligomers having a molecular weight of the order of thousands (Fig. 7). Their molecular weight does not change as the oxidation proceeds. Only after the reaction time $t = 35$ min, polymers are produced in the second oxidation step. This is illustrated by the shoulder of the molecular weight distribution extending into the region of high molecular weights (Fig. 7). Oligomer products are still present in samples collected in the end of oxidation. This indicates that oligomers have not been converted to polymers but only accompany them.

3.4. Separation by solubility in chloroform

The product collected in the early stages of aniline oxidation, $t = 3$ min, is only partly soluble in chloroform (24.8 wt.%). When the chloroform solution was evaporated on a silicon support, the square cross-like and branched crystals have been observed. This means that similar objects of 2–3 μm^2 size, observed in Figs. 4B,5A,6A, are composed of oligomers and not by polymers.

The final oxidation products typically contain both oligomeric and polymeric components (Fig. 7). We have attempted to separate them by extraction of the oligomeric fraction with chloroform. GPC in *N*-methylpyrrolidone proves that the fraction of the oxidation product soluble in chloroform (14.6 wt.%) has an oligomeric nature (Fig. 8). Some oligomers, however, are still entrapped in the chloroform-insoluble fraction.

3.5. Sulfur in polyaniline

Sulfur is present in all the PANI bases collected during synthesis (Fig. 9). The content of sulfur in the samples increases with the reaction time. It is much higher than in the standard PANI prepared in the presence of strong acids [31], 0.3 wt.%, and it has often been neglected in the literature [33]. Please note a certain similarity between Fig. 9 and the temperature profile in Fig. 3; this means that the sulfur content increases during the exothermic oxidation phases, as expected.

Support for the occurrence of sulfonation is found in the FTIR spectra. Sulfonate groups attached to the aromatic rings have been identified by the absorption peaks [39] at 1040 and 695 cm^{-1} (Fig. 10). These bands correspond to the S=O and S–O stretching vibration modes. The presence of these bands in the spectra of alkali-treated samples confirms that sulfonate groups are covalently bonded to the reaction intermediates during reaction, and not only on the completed oligomer or polymer. It seems that aniline molecules present at low acidity can also be sulfonated to *o*-aminobenzenesulfonic acid, which

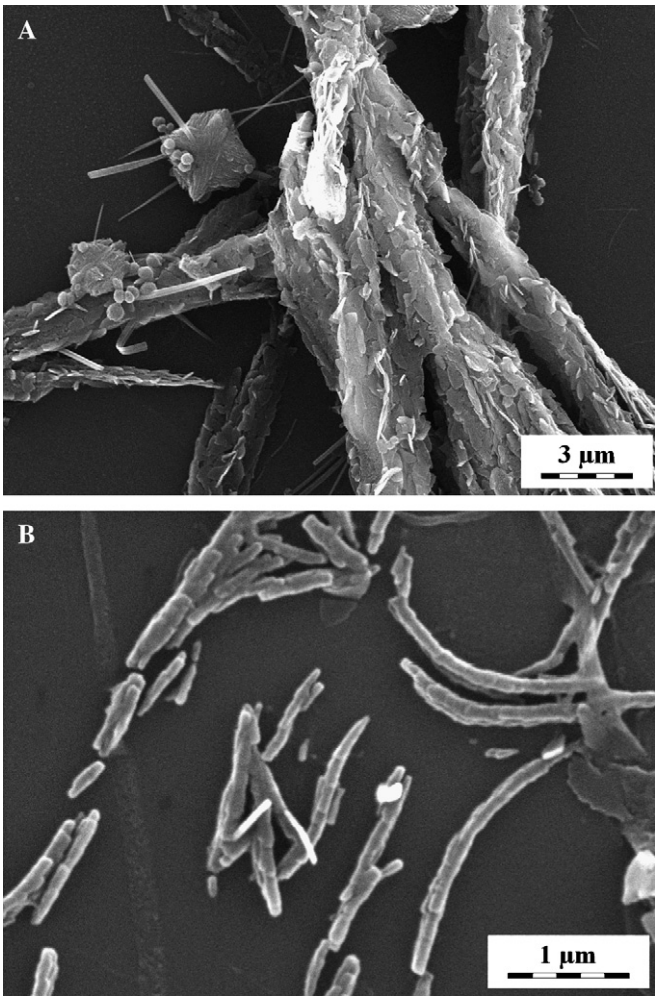

Fig. 5. SEM images of the oligomeric products obtained on silicon windows after the reaction time $t = 5$ min. Two magnifications (A,B).

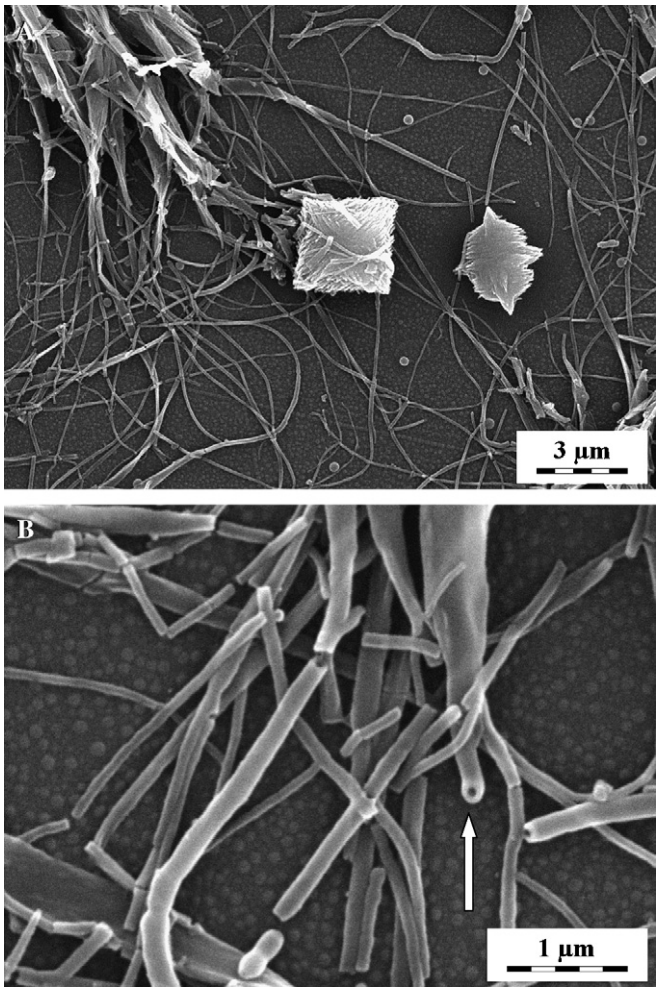

Fig. 6. SEM images of the polyaniline nanotubes produced on silicon windows after the reaction time $t = 34$ min. The internal cavity of a nanotube is marked by an arrow at the bottom micrograph. Two magnifications (A,B).

is subsequently copolymerized with aniline [40]. The sulfonate groups interact with protonated imine nitrogens in neighbouring chains and thus stabilize the supramolecular structure produced by PANI by ionic bonding [40,41].

3.6. Conductivity

Conductivity is a key parameter for this type of polymers; for typical PANI it attains the values of units S cm^{-1} [2,31]. The oligomeric products isolated in the early stages of oxidation in 0.4 M acetic acid are non-conducting, having the conductivity 2.4×10^{-10} S cm^{-1}, the conductivity of product after the completion of reaction is 0.078 S cm^{-1}. The reduced conductivity is a consequence of the two-component nature of the product composed of non-conducting oligomers and conducting PANI.

4. Discussion

4.1. Historical background

In 1856, Perkin oxidized the crude aniline, containing some toluidines, with potassium dichromate [42]. In addition to a black precipitate [42,43] (most likely, a mixture of aniline black and PANI in present terminology [44–46]), he was able to extract a purple dye, mauveine (Fig. 11A), the first

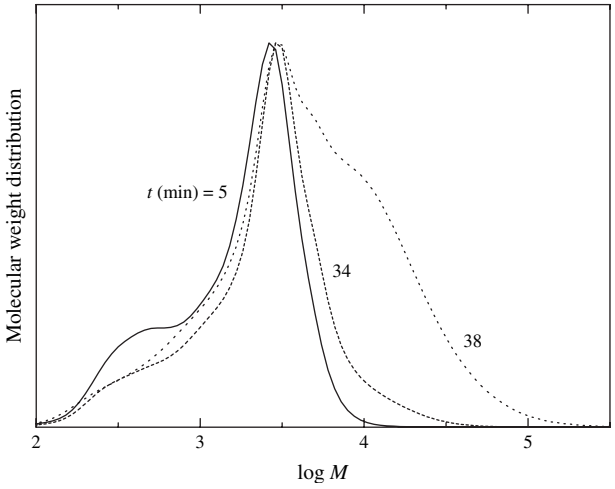

Fig. 7. Weight distributions of molecular weights M (normalized to a peak value) of the intermediates in the oxidation of aniline obtained after reaction times $t = 5$ (full line), 34 (dashed line), and 38 min (dotted line).

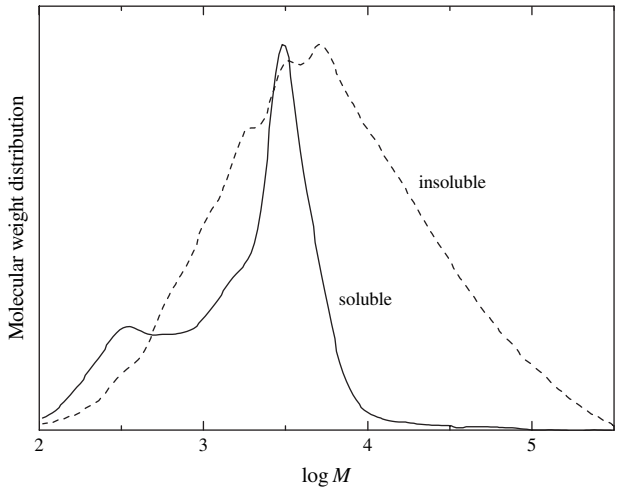

Fig. 8. Weight distributions of molecular weights M (normalized to a peak value) of the chloroform-soluble (full line) and chloroform-insoluble (dashed line) fractions of the final oxidation product.

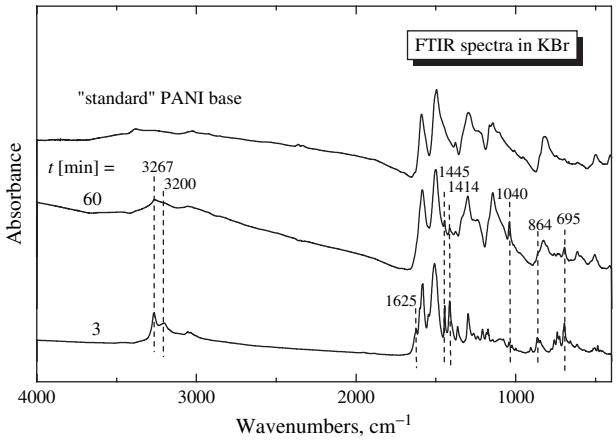

Fig. 10. FTIR spectra of samples collected at the beginning of aniline oxidation in acetic acid, $t = 3$ min, and of the final product, at $t = 60$ min. The spectrum of the PANI base, corresponding to its standard preparation in the acidic medium [31], is shown for comparison.

industrially produced dyestuff. The later oxidation of pure aniline reported in 1896 led to pseudomauveine [43] (Fig. 11B). This means that soluble protonated phenazinium structures are produced during the oxidation of aniline, and non-protonated phenazine units have been suggested as a major component in the insoluble polymeric product, aniline black [47,48] and in PANI [49]. The generation of phenazine units in PANI has also been predicted by semi-empirical quantum chemical calculations [28], and often been reported to be a result of ageing processes in PANI [50–54].

4.2. The principles of aniline oxidation

The oxidation of aniline in solutions of strong acids is the currently accepted method for preparing a conducting polymer, *i.e.*, PANI [1,2,31]. Under these reaction conditions, aniline is present as an anilinium cation, and its oxidation leads to PANI in which the aniline constitutional units are linked with a strong preference for the *para*-positions [1,54] (Fig. 1). This is generally accepted in all the proposed reaction mechanisms [1,29,55–57] and also experimentally confirmed by the oxidation of PANI to *p*-quinone [50]. Such PANI has good conductivity and, although the reaction conditions have been widely varied in the search for conductivity improvement [58,59], the high acidity of the medium has been maintained as a rule.

Oxidation started in mildly acidic [60] or even in alkaline medium [27,61] proceeds more easily [62] compared with strongly acidic media. Quantum chemical calculations have shown that aniline, which is present at pH > 4.6 mainly as a neutral molecule, is more readily oxidized than the anilinium cation [28]. These calculations also show the importance of *ortho*-coupling besides the prevalent *para*-coupling of the aniline molecules (Fig. 12A).

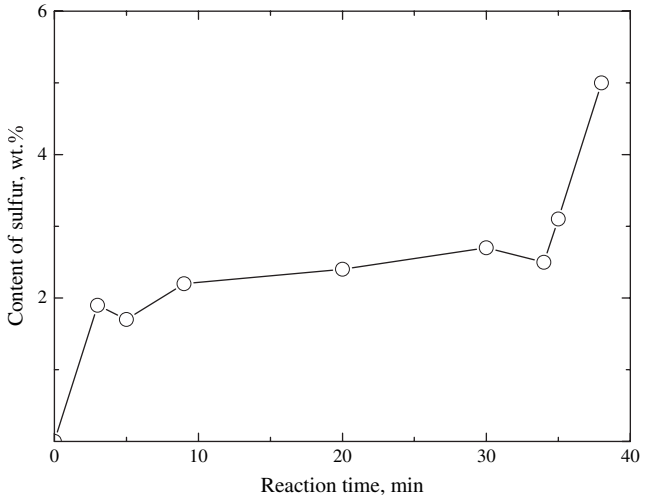

Fig. 9. The content of sulfur in the product of aniline oxidation in 0.4 M acetic acid collected after specified reaction time and deprotonated with 1 M ammonium hydroxide.

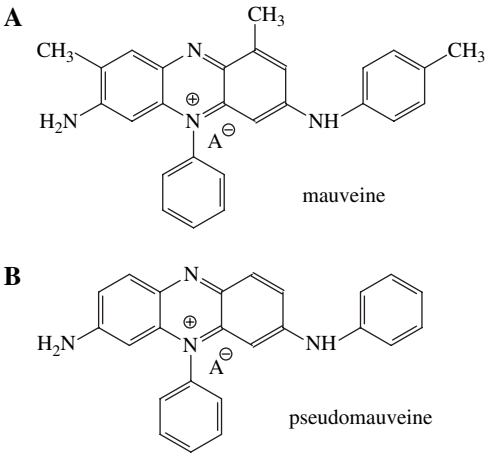

Fig. 11. (A) Mauveine, the first industrially produced synthetic dyestuff, and (B) pseudomauveine [42].

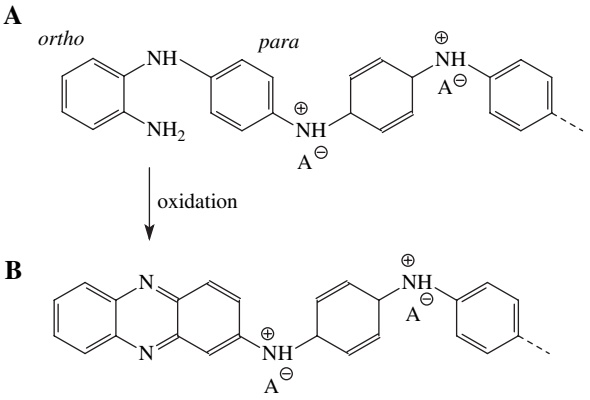

Fig. 12. (A) During the oxidation in mildly acidic media, aniline molecules couple in both the *ortho*- and *para*-positions. (B) Further oxidation of *ortho*-coupled units yields a phenazine unit, *e.g.*, at the beginning of the PANI chain [28].

The presence of *ortho*-coupled aniline molecules [63,64] in the early oxidation products resembles the situation in the oxidation of *o*-phenylenediamine [65]. Its electrochemical polymerization results in PANI-like chains with pendant amino groups but, under acidic conditions, ladder-like units of the phenazine type (Fig. 12B) were produced preferentially [66]. As the oxidation of aniline proceeds, the pH gradually decreases (Fig. 3), and this is the reason why the conversion of *ortho*-coupled aniline molecules to phenazine units is initiated (Fig. 12B). The oxidation of *o*-aminodiphenylamine, an intermediate of aniline oxidation, also yields oligomers comprising phenazine units as components [67]. When aniline has been oxidized in the media of various acidity, the initial oxidation products had optical absorption with a maximum at 370 nm [30,33], shifting to the 500 nm region, which could be assigned to the increasing conjugation in the oligomers [68] or to the formation of phenazine structures [69].

The newly produced phenazine units, or their segments, may act as initiation centres for the growth of conventional PANI, subject to the condition that pH < 2 and the intermediate pernigraniline units become protonated. Once growth starts, the aniline constitutional units are linked in the *para*-positions, due to the formation of the conducting conjugated system represented by protonated pernigraniline [25]. The propagation proceeds with a preference over initiation of PANI chains, as is illustrated by the high molecular weight of the products (Fig. 7). The resulting chains are thus expected to have a phenazine head segment and a tail of *para*-linked aniline constitutional units (Fig. 12B).

4.3. Phenazine structures in FTIR spectra

The spectrum of the final oxidation product is close to the spectrum of the PANI base prepared by a conventional method in solutions of strong acids [31] (Fig. 10). Some additional peaks are marked by dashed lines in the spectrum of the final product prepared in 0.4 M acetic acid. They are well distinguished in the spectrum of aniline oligomers (Fig. 10) and can be assigned to phenazine units (Fig. 12B). The band at 1625 cm^{-1} corresponds to the absorption of the C=C ring-stretching vibration in newly-formed substituted phenazine-like segments [70] together with the band observed at 1414 cm^{-1}, attributable to a totally symmetric stretching of the phenazine heterocyclic ring [71,72]. Phenazine-like units can also be recognized through the bands at 1208 cm^{-1} and by their contribution to the bands at 1144 and 1108 cm^{-1}. The presence of significant amount of 1,2,4-trisubstituted rings, indicative of the formation of branched and/or substituted phenazine-like segments, is revealed by the bands [41] at 864 and 858 cm^{-1}. The peaks attributable to phenazine units are more pronounced in the oligomers produced at the beginning of polymerization [35] (Fig. 10). We suppose that these peaks are overlapped by the spectrum of the newly formed *para*-coupled chains, which are generated in large excess.

4.4. Hydrogen bonding

The two relatively strong bands in the FTIR spectra, with maxima at 3267 and 3200 cm^{-1} (Fig. 10), have often been attributed to different types of intra- and inter-molecular hydrogen-bonded N–H stretching vibrations of secondary amines, N–H···N [73]. Hydrogen bonding in N–H···O, where oxygen atom belongs to a sulfonate group (discussed in Section 3.5), is also possible [35,74–77]. The presence of hydrogen bonding is indicative of the self-organization of PANI chains into supramolecular assemblies, like thin films [78–81] and nanotubes [24]. They are not found in the spectra of PANI having the common granular morphology, and seem to be associated here with the presence of nanotubes.

5. The concept of nanotube formation

5.1. Aniline oxidation

The following scenario is offered: aniline oxidation, which starts in mildly acidic conditions, at pH > 4, results in the coupling of aniline molecules in *ortho*- and *para*-positions to produce oligomers having, on average, 50–60 constitutional units. They are non-conducting. As the acidity increases, the newly *ortho*-coupled units become oxidized to phenazine units. The growth of oligomer chains proceeds to yield polymer chains at still higher acidity, pH < 2, when the intermediate pernigraniline unit can be protonated. This is reflected in the fast exothermic polymerization of aniline, producing long PANI chains.

Under highly acidic conditions, pH ~ 0–1, which are typical for PANI preparation, the proportion of phenazine participation is reduced in favour of the formation of *para*-coupled chains, which are generated in large excess. Moreover, the phenazine units become protonated [82], $pK_a = 1.2$.

5.2. Nucleation of nanotubes

The aniline oligomers produced in the early stages of oxidation are insoluble in the reaction medium; the solubility of

aniline dimers, semidines, is low [60]. Oligomers precipitate, often with frequent needle-like crystallite offsprings (Fig. 5A, upper left corner). These crystallites serve as templates for the future nucleation of PANI nanotubes.

When the acidity of the reaction mixture becomes sufficiently high, the phenazine units may initiate the propagation of polymer chains. Due to their flat structure, such hydrophobic units adsorb on the available surfaces. On solid surfaces, they nucleate the growth of PANI thin films [83,84] or the coatings of microparticles [85]. When adsorbed on added water-soluble polymer, they start the growth of colloidal dispersion particles [86,87]. The walls of the oligomer needle-like crystals similarly act as sites for the adsorption of the phenazine entities.

Various crystals present in the reaction mixture become coated with a thin conducting polymer film [21], similarly as macroscopic surfaces [88,89], or serve as centres for PANI growth [60]. The coating with PANI depends on the nature of the surface. The adsorption of phenazine units at the surface of needle-like oligomer offsprings is selective, due to the obvious anisotropy of the crystallites. We assume that the phenazine units are adsorbed on the walls of oligomer crystallites, leaving the front surfaces uncoated. In this way, the nucleus of the nanotubes is produced as a sleeve on an oligomer needle. The size of the crystallite inside determines the inner diameter of the future nanotube. Nanotubular structures with a rectangular hole, obviously produced by this mechanism, have been reported in the literature [90], and support this mechanism. The thickness of the nanotube wall corresponds to the thickness of the deposited PANI film, *e.g.*, on glass [84] $\sim$100 nm, and is proportional to the molecular weight of the PANI chains [91], *i.e.* to their extended chain length. The front surfaces of this nanotubular nucleus have exposed phenazine units adjacent to the crystallite front.

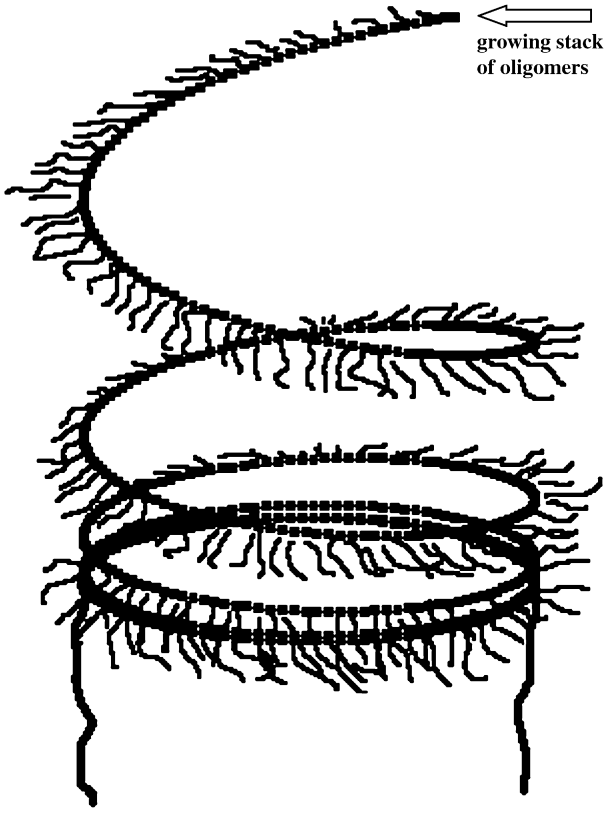

Fig. 13. The phenazine units at the start of PANI chains (squares) stack on each other, and PANI chains extend from them. The individual spiral threads are shown as being separated just for the clarity of illustration, we believe, however, that each thread closely copies the previous one and there is no separation between them. Hydrogen bonding and ionic interactions between the chains in the neighbouring threads stabilize the nanotubular structure. The oligomer crystallites nucleate the growth but the nanotube grows on its own without any external template.

5.3. The growth of a nanotube

In addition to their hydrophobic character promoting phase separation, phenazine derivatives (Fig. 12B) have a flat molecular structure that is able to produce columnar aggregates supported by $\pi-\pi$ electron interactions [92,93]. The newly produced phenazine units thus add to the exposed units at the nanotubular nucleus (Fig. 13). The PANI chains are growing from them in the preferred direction given by molecular geometry (Fig. 12B). Assembly of the terminal phenazine units thus binds the PANI chain-beginnings together. The self-ordering produced is further stabilized during the chain growth of PANI counterparts by hydrogen bonding and ionic interactions. That is why the nanotube continues to grow without any guide and with an internal cavity determined by nucleus size. This concept can be supported by the observation of nanotubular growth in polycarbonate membranes, which continue to grow beyond the membrane limits, still preserving the nanotubular morphology [94].

The growth of one-dimensional structures can also be initiated without any template. In this case, we assume that phenazine terminal units associate with each other more loosely. Stacks of one-dimensional fibrils of phenosafranines (including phenazine structures) of 1 nm diameter, which corresponds approximately to the size of a phenazine heterocycle [95], have been reported in the literature [69]. PANI chains extending from them produce a brush. A nanorod or nanowire without an internal cavity is produced instead of a nanotube. Such nanorods are observed to accompany the nanotubes (Fig. 2), and their mutual proportions are likely to be pH-dependent. At pH < 2, the phenazine heterocycles become protonated [82], the resulting phenazinium units are hydrophilic, and their ability to guide the self-ordering of polymer chains is lost. The common granular morphology of PANI is then produced [31].

The concept of soft templates, currently used in the literature [6,11,12,16], assumes the existence of micelles produced by aniline salts and the growth of PANI chains in such micellar structures. In this sense, the present model is similar in that it assumes the presence of a suitable template for the production of a nucleation site. The template nature, however, is proposed to be different, being produced by aniline oligomers rather than by a monomer. The salts of aniline with bulky organic acids [16], which may have limited solubility and crystallize

from the reaction medium, may produce a suitable template for the start of nanotubular growth [21].

5.4. The role of PANI conductivity in the polymerization of aniline

Another point is pertinent for the discussion of nanotubular growth. The oxidation of aniline to PANI is a redox process, in which the electrons are abstracted from aniline molecules and transferred to an oxidant. Peroxydisulfate accepts the electrons and converts to sulfate (Fig. 1). When PANI is produced, being a conducting polymer, it mediates the transfer of electrons between the aniline molecule and an oxidant [96]. This means that the aniline constitutional unit which is added to the growing end of a PANI nanotube can be oxidized, not only by the peroxydisulfate molecule in the vicinity, but also by *any* oxidant molecule that is close to the whole growing nanotube; the electrons are transferred through the conducting body of the already-produced PANI nanotube, without the necessity for oxidant and aniline molecules to meet directly. The probability that the PANI nanotube will grow thus increases with its length or, more generally, the mass of the produced PANI. It is thus much higher than the probability of aniline oxidation outside such a structure, which would lead to the nucleation of a new nanotube. This mechanism explains the auto-acceleration effect in aniline polymerization [56,57,97], and the topological connectivity of the PANI structure that is produced.

6. Conclusions

Polyaniline obtained by the chemical oxidation of aniline is produced in various morphologies. The reaction mechanism changes according to the acidity, which increases during the oxidation. The oxidation of neutral aniline molecules at moderate acidity, $pH > 4$, results in the formation of oligomers. They are composed of aniline constitutional units linked in both *ortho*- and *para*-positions. At higher acidity, neutral aniline molecules become protonated to anilinium cations, which are more difficult to oxidize but yield similar products. The oxidation of *ortho*-coupled units at higher acidity produces phenazine structures. These are adsorbed at the available surfaces and self-organize. It is proposed that they initiate the growth of PANI chains at $pH < 2$; a protonated pernigraniline intermediate is then produced. Chain growth proceeds with a strong preference for the coupling of aniline constitutional units in the *para*-positions.

It is proposed that needle-like oligomer crystallites serve as template sites for the growth of nanotubes after they become coated with PANI. Nanotubular growth proceeds beyond the template nucleus, without any external guide. The terminal phenazine units self-assemble and guide the growth of PANI chains, thus producing a nanotube wall. Once the tubular growth has started, each thread of the produced spiral copies the previous one. Hydrogen bonding and ionic interactions between the neighbouring PANI chains stabilize the supramolecular nanotubular structure.

Acknowledgments

The authors thank the Grant Agency of the Academy of Sciences of the Czech Republic (A4050313 and A400500504) and the Ministry of Education, Youth, and Sports of the Czech Republic (ME 847), and the Federal Agency for Science and Innovations (2005 RI-12.0/004/028) for the financial support. Thanks are due to J. Hromádková from the Institute of Macromolecular Chemistry and to M. Cieslar from Charles University in Prague for the microscopic characterization of samples and to G. Ćirić-Marjanović from the University of Belgrade for helpful comments.

References

[1] Geniès EM, Boyle A, Lapkowski M. Synth Met 1990;36:139.
[2] Trivedi DC. In: Nalwa HS, editor. Handbook of organic conductive molecules and polymers, vol. 2. Chichester: Wiley; 1997. p. 505–72.
[3] Quadrat O, Stejskal J. J Ind Eng Chem 2006;12:352.
[4] Huang J, Wan M. J Polym Sci Part A Polym Chem 1999;37:1277.
[5] Long Y, Zhang L, Ma Y, Chen Z, Wang N, Zhang Z, et al. Macromol Rapid Commun 2003;24:938.
[6] Zhang Z, Wei Z, Zhang L, Wan M. Acta Mater 2005;53:1373.
[7] Konyushenko EN, Stejskal J, Šeděnková I, Trchová M, Sapurina I, Cieslar M, et al. Polym Int 2006;55:31.
[8] Zhang X, Manohar SK. J Am Chem Soc 2005;127:14156.
[9] Zhang X, Goux WJ, Manohar SK. J Am Chem Soc 2004;126:4502.
[10] Zhang XY, Kolla HS, Wang XH, Raja K, Manohar SK. Adv Funct Mater 2006;16:1145.
[11] Chiou N-R, Epstein AJ. Adv Mater 2005;17:1679.
[12] Huang K, Wan M, Long Y, Chen Y, Wei Y. Synth Met 2005;155:495.
[13] Huang J. Pure Appl Chem 2006;78:15.
[14] Kan J, Zhang S, Jing G. J Appl Polym Sci 2006;99:1848.
[15] Li D, Kaner RB. J Am Chem Soc 2006;128:968.
[16] Zhang L, Zhang L, Wan M, Wei Y. Synth Met 2006;156:454.
[17] Stejskal J, Špírková M, Riede A, Helmstedt M, Mokreva P, Prokeš J. Polymer 1999;40:2487.
[18] Chattopadhyay D, Chakraborty M, Mandal BM. Polym Int 2001;50:538.
[19] McCarthy PA, Huang J, Yang S-C, Wang H-L. Langmuir 2002;18:259.
[20] Jing X, Wang Y, Wu D, She L, Guo Y. J Polym Sci Part A Polym Chem 2004;44:1014.
[21] Diez I, Tauer K, Schulz B. Colloid Polym Sci 2004;283:125.
[22] Diez I, Tauer K, Schulz B. Colloid Polym Sci 2006;284:1431.
[23] Zhang Z, Wei Z, Wan M. Macromolecules 2002;35:5937.
[24] Zhang L, Long Y, Chen Z, Wan M. Adv Funct Mater 2004;14:693.
[25] Fu Y, Elsenbaumer RL. Chem Mater 1994;6:671.
[26] Sbaite P, Huerta-Vilca D, Barbero C, Miras MC, Motheo AJ. Eur Polym J 2004;40:1445.
[27] Gospodinova N, Mokreva P, Terlemezyan L. Polymer 1993;34:2438.
[28] Ćirić-Marjanović G, Trchová M, Stejskal J. Collect Czech Chem Commun 2006;71:1407.
[29] Ding Y, Padias AB, Hall Jr HK. J Polym Sci Part A Polym Chem 1999;37:2569.
[30] Neoh KG, Kang ET. Polymer 1993;34:3921.
[31] Stejskal J, Gilbert RG. Pure Appl Chem 2002;74:857.
[32] Palaniappan S, Saravanan C, John A. J Macromol Sci Pure Appl Chem A 2005;42:891.
[33] Venancio EC, Wang P-C, MacDiarmid AG. Synth Met 2006;156:357.
[34] Stejskal J, Kratochvíl P, Jenkins AD. Collect Czech Chem Commun 1995;36:4135.
[35] Trchová M, Šeděnková I, Konyushenko EN, Stejskal J, Holler P, Ćirić-Marjanović G. J Phys Chem B 2006;110:9461.
[36] Kolla HS, Surwade SP, Zhang X, MacDiarmid AG, Manohar SK. J Am Chem Soc 2005;127:16770.

[37] Pillalamarri SK, Blum FD, Tokuhiro AT, Story JG, Bertino MF. Chem Mater 2005;17:227.
[38] Cheng D, Ng S-C, Chan HSO. Thin Solid Films 2001;477:15.
[39] Şahin Y, Pekmez K, Yıdız A. Synth Met 2002;131:7.
[40] Yang C-H, Chih YK, Cheng H-E, Chen C-H. Polymer 2005;46:10688.
[41] Socrates G. Infrared and Raman characteristic group frequencies. New York: Wiley; 2001. p. 78–167.
[42] Meth-Cohn O, Smith M. J Chem Soc Perkin Trans 1994;1:5.
[43] Meth-Cohn O, Travis AS. Chem Br 1995;31:547.
[44] Cao Y, Andreatta A, Heeger AJ, Smith P. Polymer 1989;30:2305.
[45] Mazeikiene R, Malinauskas A. Synth Met 2000;108:9.
[46] Ayad MM, Shenashin MA. Eur Polym J 2004;40:197.
[47] Green AG, Johnson W. Ber 1913;46:3769.
[48] Hedayatullah M. Bull Soc Chim Fr 1972;7:2957.
[49] Geniès EM, Lapkowski M, Penneau JF. J Electroanal Chem 1988;249:97.
[50] Mathew R, Mattes BR, Espe MP. Synth Met 2002;131:141.
[51] Chen C-H. J Appl Polym Sci 2003;89:2142.
[52] Cruz-Silva R, Romero-García J, Angulo-Sánchez JL, Flores-Loyola E, Farias MH, Castillón FF, et al. Polymer 2004;45:4711.
[53] Trchová M, Matějka P, Brodinová J, Kalendová A, Prokeš J, Stejskal J. Polym Degrad Stab 2006;91:114.
[54] Chen L, Yu Y, Mao H, Lu X, Zhang W, Wei Y. Synth Met 2005;149:129.
[55] Wei Y, Tang X, Sun Y. J Polym Sci Part A Polym Chem 1989;27:2385.
[56] Wei Y, Sun Y, Tang X. J Phys Chem 1989;93:4878.
[57] Geng Y, Li J, Sun Z, Jing X, Wang F. Synth Met 1998;96:1.
[58] Stejskal J, Hlavatá D, Holler P, Trchová M, Prokeš J, Sapurina I. Polym Int 2004;53:294.
[59] Blinova NV, Stejskal J, Trchová M, Prokeš J. Polymer 2006;47:42.
[60] Cases F, Huerta F, Garcés P, Morallón E, Vázquez JL. J Electroanal Chem 2001;501:186.
[61] Wang X, Liu N, Yan X, Zhang W, Wei Y. Chem Lett 2005;34:42.
[62] Liu X-X, Zhang L, Li Y-B, Bian L-J, Su Z, Zhang L-J. J Mater Sci 2005;40:4511.
[63] Zimmermann A, Künzelmann U, Dunsch L. Synth Met 1998;93:17.
[64] Cruz-Silva R, Ruiz-Flores C, Arizmendi L, Romero-García J, Arias-Marin E, Moggio I, et al. Polymer 2006;47:1563.
[65] Ichinohe D, Muranaka T, Kise H. J Appl Polym Sci 1998;70:717.
[66] Tu X, Xie Q, Xiang C, Zhang Y, Yao S. J Phys Chem B 2005;109:4053.
[67] Cotarelo MA, Huerta F, Mallavia R, Morallón E, Vázques JL. Synth Met 2006;156:51.
[68] Laska J, Widlarz J. Polymer 2005;46:1485.
[69] Komura T, Ishihara M, Yamaguchi T, Takahashi K. J Electroanal Chem 2000;493:84.
[70] Li X-G, Duan W, Huang M-R, Yang Y-L. J Polym Sci Part A Polym Chem 2001;39:3989.
[71] Viva FA, Andrade EM, Molina FV, Florit MI. J Electroanal Chem 1999;471:180.
[72] Dines TJ, MacGregor LD, Rochester CH. Phys Chem Chem Phys 2001;13:2676.
[73] Holly S, Sohár P. In: Láng L, Prichard WH, editors. Absorption spectra in the infrared region (theoretical and technical introduction). Budapest: Akadémiai Kiadó; 1975. p. 69.
[74] Vien DL, Colthup NB, Fateley WG, Grasselli JG. The handbook of infrared and Raman characteristic frequencies of organic molecules. New York: Academic Press; 1991.
[75] Kieffel Y, Travers JP, Ermolieff A, Rouchon D. J Appl Polym Sci 2002;86:395.
[76] Lin X, Zhang H. Electrochim Acta 1996;41:2019.
[77] Coates J. Encyclopedia of analytical chemistry. In: Meyers RA, editor. Interpretation of infrared spectra: a practical approach. Chichester: Wiley; 2000. p. 10815–37.
[78] Trchová M, Sapurina I, Prokeš J, Stejskal J. Synth Met 2003;135–136:305.
[79] Wu G-C, Yeh Y-R, Chen J-Y, Chiou Y-H. Polymer 2001;42:2877.
[80] Sapurina I, Osadchev AYu, Volchek BZ, Trchová M, Riede A, Stejskal J. Synth Met 2002;129:29.
[81] Šeděnková I, Trchová M, Blinova NV, Stejskal J. Thin Solid Films 2006. doi:10.1016/j.tsf.2006.05.038.
[82] Inzelt G, Puskas Z. Electrochim Acta 2004;49:1969.
[83] Malinauskas A. Polymer 2001;42:3957.
[84] Stejskal J, Sapurina I. Pure Appl Chem 2005;77:815.
[85] Okubo M, Fujii S, Minami H. Colloid Polym Sci 2001;279:139.
[86] Stejskal J. J Polym Mater 2001;18:225.
[87] Stejskal J, Sapurina I. J Colloid Interface Sci 2004;274:489.
[88] Wang P-C, Huang Z, MacDiarmid AG. Synth Met 1999;101:852.
[89] Onoda M, Tada K, Shinkuma A. Thin Solid Films 2006;499:61.
[90] Li G, Pang S, Xie G, Wang Z, Peng H, Zhang Z. Polymer 2006;47:1456.
[91] Stejskal J, Riede A, Hlavatá D, Prokeš J, Helmstedt M, Holler P. Synth Met 1998;96:55.
[92] Crispin X, Cornil A, Friedlein R, Okudaira KK, Lemaur V, Crispin A, et al. J Am Chem Soc 2004;126:11889.
[93] Kokunov YV, Gorbunova YE, Khmelevskaya LV. Russ J Inorg Chem 2005;50:1184.
[94] Tagowska M, Palys B, Jackowska K. Synth Met 2004;142:223.
[95] Sáez EI, Corn RM. Electrochim Acta 1993;38:1619.
[96] Kocherginsky NM, Lei W, Wang Z. J Phys Chem A 2005;109:4010.
[97] Tzou K, Gregory RV. Synth Met 1992;47:267.